

# Hyperbranched Polymer Functionalized Carbon Dots with Multistimuli-Responsive Property

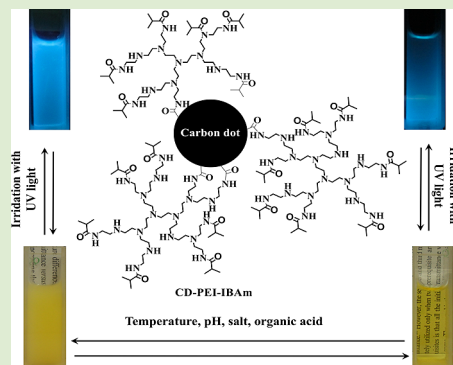
Jing-Yuan Yin,<sup>†</sup> Hua-Ji Liu,<sup>†</sup> Songzi Jiang,<sup>‡</sup> Yu Chen,<sup>\*,†</sup> and Yefeng Yao<sup>\*,‡</sup>

<sup>†</sup>Department of Chemistry, School of Sciences, Tianjin University, Tianjin 300072, People's Republic of China

<sup>‡</sup>Department of Physics & Shanghai Key Laboratory of Magnetic Resonance, East China Normal University, North Zhongshan Road 3663, Shanghai 200062, People's Republic of China

## S Supporting Information

**ABSTRACT:** The pyrolysis of a hyperbranched polyethylenimine (PEI) and glycerol mixture under microwaves generated the carbon dot (CD) functionalized with PEI (CD-PEI). Isobutyric amide (IBAm) groups were attached to CD-PEI through the amidation reaction of isobutyric anhydride and the PEI moiety, which resulted in the thermoresponsive CD-PEI-IBAm's. CD-PEI-IBAm's were not only thermoresponsive but also responded to other stimuli, including inorganic salt, pH, and loaded organic guests. The cloud point temperature ( $T_{cp}$ ) of the aqueous solutions of CD-PEI-IBAm's could be modulated in a broad range through changing the number of IBAm units of CD-PEI-IBAm or varying the type and concentration of the inorganic salts, pH, and loaded organic guests. All the obtained CD-PEI-IBAm's were photoluminescent, which could be influenced a little or negligibly by the added salts, pH, and the organic guests encapsulated.



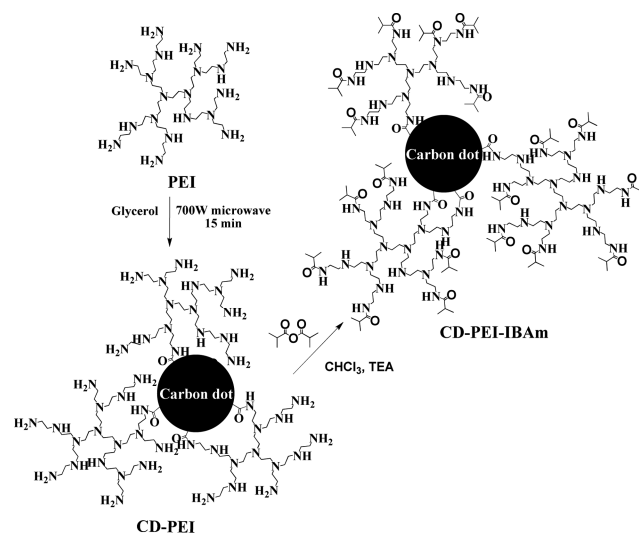
During the past decade, carbon dots (CDs), which are discrete quasi-spherical nanoparticles with sizes less than 10 nm and display size and excitation wavelength dependent photoluminescence behavior, have attracted much interest.<sup>1,2</sup> CDs are versatile and possess distinct merits, such as a simple fabrication process, low production cost, chemical inertness, a lack of optical blinking, low photobleaching, low cytotoxicity, and excellent biocompatibility. These particular characters endow CDs enormous potential applications, such as bioimaging,<sup>3–7</sup> photocatalysis,<sup>8,9</sup> sensing,<sup>10–13</sup> lasers,<sup>14</sup> light-emitting diodes,<sup>15</sup> and ink.<sup>16</sup>

Thermoresponsive polymers with a lower critical solution temperature (LCST) in aqueous solution have attracted much interest<sup>17</sup> and are frequently utilized to endow the luminescent materials with thermoresponsive property. Beyond the vast single thermostimulus-responsive photoluminescent materials, a few with dual stimuli-responsive property have been addressed.<sup>18–21</sup> Nonetheless, multifunctional photoluminescent materials that respond to more than two stimuli have seldom been prepared.<sup>22</sup> Up to present date, only a few polymeric reagents have been employed as passivating agents for the luminescent CDs, such as hyperbranched polyethylenimine (PEI),<sup>4</sup> diamine-terminated oligomeric poly(ethylene glycol),<sup>23,24</sup> poly(propionylethylenimine-co-ethyleneimine),<sup>23</sup> and polyaniline.<sup>25</sup> However, to our best knowledge, CDs with superior biocompatibility and resistance to photobleaching have never been integrated with thermoresponsive polymers. Herein, we report a multistimuli-responsive CD integrated with thermoresponsive hyperbranched polymers that is sensitive to temperature, inorganic ions, pH, and organic compounds. Furthermore, such a CD is not only photoluminescent but also

able to host guest molecules as a nanocarrier. Hence, it is possible for such a CD to be used as a drug-delivery system with the self-bioimaging function.

The multistimuli-responsive CD was prepared by two steps (Scheme 1). First, the pyrolysis of the PEI and glycerol

## Scheme 1. Preparation of Multistimuli-Responsive Carbon Dot



Received: September 12, 2013

Accepted: October 2, 2013

Published: November 8, 2013

**Table 1. Structural Information of Thermo-responsive CD-PEI-IBAm's and Their Phase Transition Temperature**

samples	CD-PEI precursor			DS <sub>(IBAm)</sub> <sup>c</sup> (%)	T <sub>cp</sub> <sup>d</sup> (°C)	mean diameter (nm)	
	PEI precursor	PEI content <sup>a</sup> (%)	degree of amidation <sup>b</sup> (%)			TEM	DLS
CD-1	PEI1.8K	71.1	31.5	44.2 (43.4)	42.7	4.0 ± 0.4	4.5
CD-2	PEI10K	70.4	20.5 (19.8)	36.9 (33.8)	46.7	4.7 ± 0.5	6.5
CD-3	PEI10K	70.4	20.5 (19.8)	44.1 (42.8)	36.7	4.6 ± 0.4	6.5
CD-4	PEI10K	70.4	20.5 (19.8)	46.2 (43.8)	34.0	4.7 ± 0.4	6.7

<sup>a</sup>Weight percentage of PEI in CD-PEI. <sup>b</sup>Degree of amidation means the mole percentage of PEI's amino groups that react with the carboxylic acid groups of the CD moiety, which is calculated from <sup>1</sup>H NMR or <sup>15</sup>N NMR (data in parentheses). <sup>c</sup>DS<sub>(IBAm)</sub> represents the mole percentage of PEI's amino groups that are substituted by IBAm units, which is calculated from <sup>1</sup>H NMR or elemental analysis (data in parentheses). <sup>d</sup>T<sub>cp</sub> represents the cloud point temperature, obtained from 24 mg/mL of aqueous solution of CD.

under 700 W microwaves for 10 min generated the PEI-functionalized CD (CD-PEI).<sup>4</sup> Second, isobutyric amide (IBAm) groups were coupled with CD-PEI through the amidation reaction of isobutyric anhydride and HPEI moiety. In the first step, two commercially available PEI samples, namely, PEI1.8K ( $M_n = 1800$  g/mol,  $M_w/M_n = 1.04$ ) and PEI10K ( $M_n = 10^4$  g/mol,  $M_w/M_n = 2.5$ ), were utilized, resulting in CD-PEI1.8K and CD-PEI10K, respectively. Before the subsequent modification, we attempted to clarify the structural information of these CD-PEI compounds. In the TEM images of CD-PEI1.8K and CD-PEI10K (Figure S1 in the Supporting Information), dark dots with average diameters of 4.0 and 4.8 nm, respectively, can be seen clearly. These dark dots have a crystalline structure consisting of parallel crystal planes with lattice spacings of 0.21 and 0.31 nm, which matches with the (100) and (002) lattice spacing of graphite,<sup>26,27</sup> verifying the successful formation of CDs. Dynamic light scattering (DLS) characterization shows that the average diameters of CD-PEI1.8K and CD-PEI10K are 4.3 and 6.1 nm, respectively, bigger than those calculated from TEM (Figure S2 in the Supporting Information). Comparing the mean diameter measured by TEM and DLS, it can be deduced that these CDs have a core-shell structure, and the core and shell are made of nanocarbon and PEI, respectively. Zeta-potential measurements show that the as-prepared CD-PEIs are positively charged ( $\zeta = 6.5$  and 28.8 mV for CD-PEI1.8K and CD-PEI10K, respectively) owing to the polycation nature of the PEI moiety. Elemental analysis demonstrates that (Table S1 in the Supporting Information) the PEI content in the obtained CD-PEIs is ca. 70% (Table 1).

FTIR characterization demonstrates that amidation reaction between PEI and CD occurs due to the very strong absorption at 1662 cm<sup>-1</sup> characteristic for the C=O stretching bond frequency of amide groups (Figure S3 in the Supporting Information). It is known that glycerol can be carbonized under microwaves to produce carboxylic acid groups that can be amidated with PEI;<sup>4</sup> however, whether PEI is stable under microwaves is unclear. Therefore, the PEI sample heated under 700 W microwaves in the absence of glycerol was also characterized by FTIR, and it was found that the FTIR spectra of PEI before and after heating under microwave were similar. Moreover, PEIs before and after heating under microwave were also characterized by <sup>13</sup>C NMR, and it was found that the degree of branching and the ratio of primary, secondary, and tertiary amines of PEI had no obvious alteration, indicating that PEI is stable under the microwave heating.

CD-PEIs were characterized by <sup>1</sup>H NMR (Figure S4A in the Supporting Information). Compared with pure PEI (Figure S4B in the Supporting Information), new signals assigned for the methylene protons attached to the amide groups can be

seen clearly between 3 and 4 ppm. In the range of 6–8 ppm, very weak peaks assigned for the protons connected with the unsaturated carbons of the CD moiety are visible. In the range of 0.5–2 ppm, weak peaks assigned for the protons connected with the saturated carbons of the CD moiety are also visible. That the signals of the CD moiety are so weak can be ascribed to its low proton content (Table S1 in the Supporting Information). From <sup>1</sup>H NMR spectra the degree of amidation relative to the total nitrogen of PEI can be calculated, and it is found that the lower molecular weight of PEI has a higher degree of amidation (Table 1). It has been known that during the formation of CDs carboxylic acid groups were generated on or in the carbon sphere.<sup>1</sup> The carboxylic acid groups on the surface were reactive and could react with both low and high molecular weight of PEIs. However, the inner carboxylic acid groups could only react with the lower molecular weight of PEIs due to the steric hindrance effect.

CD-PEI was further characterized by <sup>13</sup>C NMR (Figure S5 in the Supporting Information). The carbon content of CD is not so low (Table S1 in the Supporting Information); however, their intensity (unsaturated carbons at around 120 ppm, ether carbons in the range of 60–70 ppm, and saturated carbons in the range of 10–30 ppm) is very weak and even invisible. Such a phenomenon can be explained as follows: CD is big and rigid, and therefore its rotational and diffusional mobility is confined seriously, leading to the weakness or even invisibility of the carbon signals. Furthermore, the amide carbon directly anchored onto the CD (at around 170 ppm) cannot be seen clearly, either, which can also be attributed to confinement of its rotational and diffusional mobility by such a big and rigid CD entity. As for the PEI moiety, except for the amide carbon that is located at the junction of CD and PEI, other carbons that are away from the CD can be seen clearly. However, compared with the pure PEI, the carbon signals of CD-PEI are broadened pronouncedly. These results demonstrate that the rotational and diffusional mobilities of PEI and CD moieties are low in the CD-PEI entity, and they are more pronounced for the big and rigid CD moiety. In the <sup>13</sup>C NMR spectrum of PEI, the carbon signals adjacent to various amino groups are separated well, thus it is possible to calculate the ratio of primary, secondary, and tertiary amino groups of PEI. In the <sup>13</sup>C NMR spectrum of CD-PEI, beyond the carbon signals adjacent to various amino groups, new  $\alpha$  and  $\beta$  carbon signals of amide appear in their upfield position, such as the signals at 56.46, 45.69, and 38.45 ppm. Since the carbon signals related with amino and amide groups are overlapped so seriously, it is not possible to calculate how many amino groups of PEI have been amidated with the CD. Overall, from <sup>13</sup>C NMR it can be only indirectly proved that PEI reacts with the CD through amidation reaction.

We also attempted to characterize CD-PEI through  $^{15}\text{N}$  NMR (Figure S6 in the Supporting Information). Just like the amide carbon in  $^{13}\text{C}$  NMR, the amide nitrogen (around  $-270$  ppm) signals cannot be seen, either. In the  $^{15}\text{N}$  NMR of CD-PEI, nitrogen signals of primary, secondary, and tertiary amines can be seen clearly, and they are also much broader than those in the pure PEI. This further proves that CD restricts the rotational and diffusional mobility of PEI, especially for the directly anchored amide groups. From the structure of PEI it can be known that the steric hindrance of secondary amines in PEI is serious, thus the reactivity of secondary amines of PEI with the big and rigid CD should be very low. It is reasonable that the amidation reaction mainly happens between primary amines of PEI and CD. Under the assumption that the amount of secondary and tertiary amines of PEI is invariable before and after reaction with the CD, we compare the nitrogen integrals of PEI and CD-PEI using the integrals of secondary plus tertiary amines as the standard, and the integral decrease of primary amines in CD-PEI is thought as the transformation into amide units. From  $^{15}\text{N}$  NMR of CD-PEI we calculate the amount of amide nitrogen, and the result is similar to that from  $^1\text{H}$  NMR (Table 1).

The residual reactive amino groups of CD-PEIs were further amidated with isobutyric anhydride to result in CD-PEI-IBAm's. FTIR shows that the intensity of the signal characteristic for the  $\text{C}=\text{O}$  stretching bond frequency of amide groups (centered at  $1639\text{ cm}^{-1}$  in Figure S3C in the Supporting Information) becomes much stronger than that of CD-PEI, indicating the successful amidation reaction between CD-PEI and isobutyric anhydride. In the  $^1\text{H}$  NMR spectrum (Figure S4C in the Supporting Information), the methyl protons of IBAm units appear at 1.09 ppm, and the methylene protons connected with IBAm occur at 3.65 ppm. From  $^1\text{H}$  NMR the degree of substitution of IBAm [ $\text{DS}_{(\text{IBAm})}$ ] relative to the total nitrogen of PEI can be calculated, which are close to the values derived from elemental analysis (Table 1 and Table S2 in the Supporting Information).

We prepared one CD-PEI1.8K-IBAm (CD-1) and three CD-PEI10K-IBAm's (CD-2, CD-3, and CD-4) with different  $\text{DS}_{(\text{IBAm})}$  values, and their average diameters measured from TEM and DLS are similar to their respective precursor (Table 1). Zeta-potential measurements show that the  $\zeta$  values of all these CDs are close to zero, indicating that the introduction of a vast number of IBAm groups severely reduces the positive charges of these CDs.

Aqueous solutions of these CD-PEI-IBAm's were yellow and transparent, which became turbid after being heated above certain temperatures and went transparent again when they were cooled (Figure S7 in the Supporting Information). This indicated that the obtained CD-PEI-IBAm's were thermoresponsive. Figure 1 depicts the typical temperature dependence of the light transmittance of aqueous solutions of these CD-PEI-IBAm's, and obvious phase transition can be seen. From Figure 1 the phase transition temperature, here called cloud-point temperatures ( $T_{\text{cp}}$ ), can be read off, and the results are listed in Table 1. It is clear that the molecular weight of PEI employed has a negligible influence on the  $T_{\text{cp}}$  (comparing CD-1 with CD-3), whereas lowering the  $\text{DS}_{(\text{IBAm})}$  value can effectively increase the  $T_{\text{cp}}$  (comparing CD-2 with CD-3). It is known that more hydrophilic polymers usually have higher  $T_{\text{cp}}$  because it requires more energy to release the hydrated water molecules from the polymers.<sup>28</sup> Relative to the amino groups of PEI, IBAm groups are hydrophobic. CD-PEI-IBAm with a

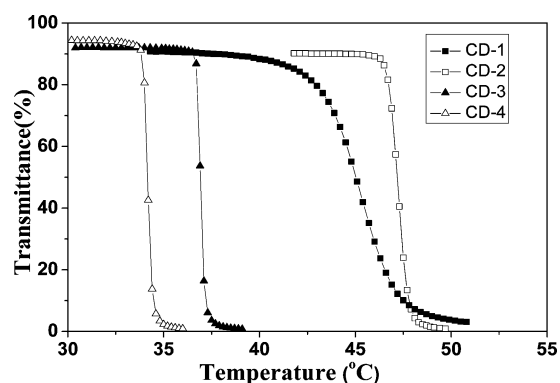


**Figure 1.** Influence of temperature on the light transmittance of CD-PEI-IBAm in deionized water (concentration of CDs is 24 mg/mL).

lower  $\text{DS}_{(\text{IBAm})}$  is therefore more hydrophilic, having a higher  $T_{\text{cp}}$ .

With CD-4 as a representative, DLS was used to monitor the size variation during the phase transition (Figure S8 in the Supporting Information). Below the transition temperature, the average diameter of CD-4 in water is always around 7 nm. When the temperature is elevated above the transition temperature, the size increases pronouncedly, indicating the occurrence of large aggregation. During the phase transition, no obvious shrinkage of the PEI-IBAm shell can be observed due to its inherent compact structure. Moreover, compared with the curve from the turbidity measurement, it can be found that the phase transition temperatures measured from the DLS and turbidity are similar.

The salt sensitivity of the thermoresponsive property of CD-PEI-IBAm was measured, and CD-4 was employed as the representative. Three sodium salts with the typical anions, including  $\text{Cl}^-$ ,  $\text{SO}_4^{2-}$ , and  $\text{I}^-$ , were chosen. The  $T_{\text{cp}}$  value of CD-4 can be modulated to different extents by the addition of different inorganic anions (Figure 2A).  $\text{I}^-$  exhibits the

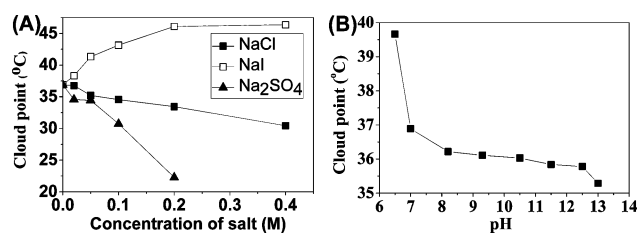


**Figure 2.**  $T_{\text{cp}}$  of CD-4 influenced by (A) different salts (■) NaCl, (□) NaI, and (▲)  $\text{Na}_2\text{SO}_4$  and (B) pH (concentration of CD-4 is 4 mg/mL).

significant salting-in effect that is embodied by the increase of  $T_{\text{cp}}$  in certain salt concentration regions, whereas  $\text{Cl}^-$  and  $\text{SO}_4^{2-}$  show the obvious salting-out effect that is embodied by the decrease of  $T_{\text{cp}}$ . Furthermore,  $\text{SO}_4^{2-}$  is more efficient to lower the  $T_{\text{cp}}$  than  $\text{Cl}^-$ . The specific ranking of these three anions in reducing the  $T_{\text{cp}}$  is  $\text{SO}_4^{2-} > \text{Cl}^- > \text{I}^-$ . This sequence is in accordance with the well-known Hofmeister series for the biopolymers and synthetic water-soluble polymers.<sup>29–31</sup> The sensitivity of CD-4 to salts is similar to the dendritic thermoresponsive polymer PEI-IBAm<sup>32,33</sup> but much higher than the linear thermoresponsive polymer PNIPAm.<sup>34</sup> For instance, concentrations of ca. 0.3 M  $\text{Na}_2\text{SO}_4$  lowered the LCSTs of linear PNIPAM around  $10\text{ }^\circ\text{C}$ , while NaI elevated its



LCST maximally about 2 (ca. 0.3 M). Whereas from Figure 2A it can be known that 0.2 M  $\text{Na}_2\text{SO}_4$  can lower the  $T_{\text{cp}}$  of CD-4 about 15 °C, 0.2 M NaI can enhance the  $T_{\text{cp}}$  of CD-4 by ca. 7 °C.

The thermoresponsive property of the obtained CD-4 is also pH-sensitive (Figure 2B). The pH of CD-4 in water is close to 7. Increasing the acidity significantly increases  $T_{\text{cp}}$ . Conversely, adjusting the pH to around 8 obviously lowers the  $T_{\text{cp}}$ . The decrease of  $T_{\text{cp}}$  becomes insignificant after increasing the pH to 12.5. After the pH reaches around 13, the  $T_{\text{cp}}$  decreases pronouncedly again. The pH response of CD-4 is interpreted as follows: As the acidity of an aqueous solution of CD-4 increases, more amino groups of CD-4 are protonated to form more polar  $\text{N}^+$  groups. The significant increase in polarity increases  $T_{\text{cp}}$ . In contrast, increasing basicity gradually turns the more polar protonated  $\text{N}^+$  groups into less polar amines, decreasing  $T_{\text{cp}}$ . When the pH is high enough, the concentration of  $\text{OH}^-$  is high enough in the system to affect the hydration waters wrapped around the CD-4.  $\text{OH}^-$  is a kosmotropic anion that dehydrates CD-4. This leads to the salting-out of CD-4, thereby lowering the  $T_{\text{cp}}$ .

PEI-IBAm can encapsulate organic molecules with a carboxylic acid group through acid–base neutralization.<sup>35,36</sup> Thus, we also studied the influence of the loaded organic compounds on the thermoresponsive property of CD-PEI-IBAm. Aspirin and pyrene-4-butyric acid (PBA) were utilized as the guest models. The successful interaction between CD-PEI-IBAm and these two guests can be interpreted from the 2D NOESY  $^1\text{H}$  NMR spectroscopy that is a powerful technique to investigate the interaction between two different components in close proximity (<0.5 nm). The 2D NOESY  $^1\text{H}$  NMR spectra of the mixtures of CD-4 with aspirin or PBA show strong positive cross-peaks between the aromatic rings of the guests and the inner methylene groups of CD-4 (Figures S9 and S10 in the Supporting Information), revealing the formation of the complex of CD-4 and aspirin or PBA. Subsequently, the thermoresponsive properties of these complexes were studied. From Figure 3 it can be seen that the relatively polar aspirin

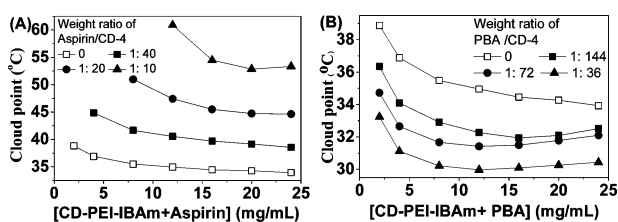


**Figure 3.**  $T_{\text{cp}}$  of CD-4 influenced by the organic additive (A) aspirin and (B) PBA.

guest can increase the  $T_{\text{cp}}$ , and increasing the content of aspirin in the complex results in the gradual increase of  $T_{\text{cp}}$ . However, loading the apolar PBA guest leads to the decrease of  $T_{\text{cp}}$ , and the more PBA molecules that are loaded, the lower the  $T_{\text{cp}}$  is.

All the obtained CD-PEI-IBAm's are photoluminescent. When temperature is lower than  $T_{\text{cp}}$ , the aqueous solutions of these CD-PEI-IBAm's irradiated with 350 nm UV light illuminate blue light, and the solutions are still transparent. When the temperature is higher than  $T_{\text{cp}}$ , the solutions become turbid and still illuminate blue light, but the emission intensity is decreased pronouncedly (Figure 4). With CD-4 as the representative, it can be seen that the emission intensity decreases about 65% when the temperature increases from 26

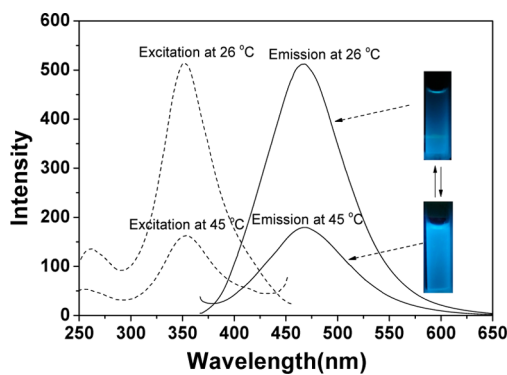


**Figure 4.** Typical excitation and emission spectra of CD-4 at room temperature (26 °C) and 45 °C (concentration of CD-4 is 2 mg/mL, inset: the typical luminescent photographs of CD-4).

to 45 °C. CD-PEI10K, the precursor of CD-4, is also luminescent, and its emission intensity also decreases upon increasing the temperature (Figure S11 in the Supporting Information). However, its emission intensity decreases only about 36% upon increasing the temperature from 26 to 45 °C. Therefore, the emission reduction of CD-4 upon increasing temperature above  $T_{\text{cp}}$  can be ascribed to two aspects: one is the inherent property of the CDs prepared by a such way and the other is due to the thermo-induced aggregation of CD particles.

The detailed photoluminescent characterization shows that the maximal excitation wavelength ( $\lambda_{\text{ex}}$ ) and emission wavelength ( $\lambda_{\text{em}}$ ) of CD-PEI-IBAm are concentration- dependent (Figure S12 in the Supporting Information). At low concentration (below 10 and 4 mg/mL for CD-4 and CD-1, respectively), the maximal  $\lambda_{\text{ex}}$  and  $\lambda_{\text{em}}$  are always around 350 and 470 nm, respectively. However, the emission intensity varies pronouncedly when the concentration of CD-PEI-IBAm varies in this concentration region (Figure S12C in the Supporting Information). The emission intensity increases upon increasing the concentration at the beginning. After reaching the maximal emission intensity at a certain concentration, it decreases with the further concentration increase. When the concentration is above the low concentration limit, both the maximal  $\lambda_{\text{ex}}$  and  $\lambda_{\text{em}}$  increase pronouncedly with the concentration increase. The emission wavelength can arrive in the region of green, even red light. However, the emission intensity is much lower than that of the strongest blue light. The increase of maximal  $\lambda_{\text{ex}}$  and  $\lambda_{\text{em}}$  and the weakening of emission at a high CD concentration might be attributed to the microscopic aggregation of CD particles.

Whether salts, pH, and the encapsulated organic molecules have an influence on the emission intensity was measured (Figure S13 in Supporting Information). It is clear that these factors have a little or even negligible influence on the emission of CD-PEI-IBAm.

In summary, multistimuli-responsive photoluminescent CDs that responded to temperature, salt, pH, and encapsulated organic guests were successfully prepared. The aqueous solutions of CD-PEI-IBAm's were thermoresponsive, and the  $T_{\text{cp}}$  could be modulated through changing the  $\text{DS}_{(\text{IBAm})}$  value of CD-PEI-IBAm. Moreover, the  $T_{\text{cp}}$  could be also tuned in a broad range through changing the pH, the type, and concentration of salts added and the type and concentration of organic guests encapsulated. Low pH, the traditional salting-in anion, and polar organic guests increased the  $T_{\text{cp}}$

pronouncedly, whereas high pH, the traditional salting-out anions, and apolar organic guest favored the decrease of  $T_{cp}$ . All the obtained CD-PEI-IBAm's were photoluminescent, which was influenced a little or negligibly by pH, salts, and the organic guests encapsulated.

CD-PEI-IBAm's integrate the multistimuli-responsive property, nanocarrier for organic guest, and luminescent property together, thus it is promising for them to be applied in the field of biomedicine and biotechnology as "smart" materials.

## ■ ASSOCIATED CONTENT

### ● Supporting Information

Experimental details; the data of elemental analysis; TEM images; DLS curves; the typical FTIR,  $^1\text{H}$ ,  $^{13}\text{C}$ , and  $^{15}\text{N}$  NMR spectra; and the typical photoluminescent spectra. This material is available free of charge via the Internet at <http://pubs.acs.org>.

## ■ AUTHOR INFORMATION

### Corresponding Authors

\*E-mail: [chenyu@tju.edu.cn](mailto:chenyu@tju.edu.cn).

\*E-mail: [yfyao@phy.ecnu.edu.cn](mailto:yfyao@phy.ecnu.edu.cn).

### Notes

The authors declare no competing financial interest.

## ■ ACKNOWLEDGMENTS

This work was financially supported by the Program for New Century Excellent Talents in University and the National Natural Science Foundation of China (20804027, 21274106).

## ■ REFERENCES

- (1) Baker, S. N.; Baker, G. A. *Angew. Chem., Int. Ed. Engl.* **2010**, *49* (38), 6726–6744.
- (2) Xu, X. Y.; Ray, R.; Gu, Y. L.; Ploehn, H. J.; Gearheart, L.; Raker, K.; Scrivens, W. A. *J. Am. Chem. Soc.* **2004**, *126*, 12736–12737.
- (3) Wang, X.; Cao, L.; Yang, S. T.; Lu, F.; Meziani, M. J.; Tian, L.; Sun, K. W.; Bloodgood, M. A.; Sun, Y. P. *Angew. Chem., Int. Ed. Engl.* **2010**, *49* (31), 5310–5314.
- (4) Liu, C.; Zhang, P.; Zhai, X.; Tian, F.; Li, W.; Yang, J.; Liu, Y.; Wang, H.; Wang, W.; Liu, W. *Biomaterials* **2012**, *33* (13), 3604–3613.
- (5) Cao, L.; Wang, X.; Meziani, M. J.; Lu, F.; Wang, H.; Luo, P. G.; Lin, Y.; Harruff, B. A.; Veca, L. M.; Murray, D.; Xie, S. Y.; Sun, Y. P. *J. Am. Chem. Soc.* **2007**, *129*, 11318–11319.
- (6) Wang, F.; Xie, Z.; Zhang, H.; Liu, C. Y.; Zhang, Y. G. *Adv. Funct. Mater.* **2011**, *21*, 1027–1031.
- (7) Liu, R.; Wu, D.; Liu, S.; Koynov, K.; Knoll, W.; Li, Q. *Angew. Chem., Int. Ed. Engl.* **2009**, *48* (25), 4598–4601.
- (8) Cao, L.; Sahu, S.; Anilkumar, P.; Bunker, C. E.; Xu, J.; Fernando, K. A. S.; Wang, P.; Gulians, E. A.; Tackett, K. N.; Sun, Y. P. *J. Am. Chem. Soc.* **2011**, *133*, 4754–4757.
- (9) Li, H. T.; He, X.; Kang, Z.; Huang, H.; Liu, Y.; Liu, J.; Lian, S.; Tsang, A. C. H.; Yang, X.; Lee, S. T. *Angew. Chem., Int. Ed. Engl.* **2010**, *49*, 4430–4434.
- (10) Zhao, H. X.; Liu, L. Q.; Liu, Z. D.; Wang, Y.; Zhao, X. J.; Huang, C. Z. *Chem. Commun.* **2011**, *47*, 2604–2606.
- (11) Wei, W.; Xu, C.; Ren, J.; Xu, B.; Qu, X. *Chem. Commun.* **2012**, *48*, 1284–1286.
- (12) Zhou, L.; Lin, Y.; Huang, Z.; Ren, J.; Qu, X. *Chem. Commun.* **2012**, *48*, 1147–1149.
- (13) Liu, S.; Tian, J.; Wang, L.; Zhang, Y.; Qin, X.; Luo, Y.; Asiri, A. M.; Al-Youbi, A. O.; Sun, X. *Adv. Mater.* **2012**, *24*, 2037–2041.
- (14) Zhang, W. F.; Zhu, H.; Yu, S. F.; Yang, H. Y. *Adv. Mater.* **2012**, *24*, 2263–2267.
- (15) Wang, F.; Chen, Y. H.; Liu, C. Y.; Ma, D. G. *Chem. Commun.* **2011**, *47*, 3502–3504.
- (16) Qu, S.; Wang, X.; Lu, Q.; Liu, X.; Wang, L. *Angew. Chem., Int. Ed. Engl.* **2012**, *51* (49), 12215–12218.
- (17) Weber, C.; Hoogenboom, R.; Schubert, U. S. *Prog. Polym. Sci.* **2012**, *37* (5), 686–714.
- (18) Chen, Y.; Li, X. *Biomacromolecules* **2011**, *12*, 4367–4372.
- (19) Uchiyama, S.; Kawai, N.; Silva, A. P. d.; Iwai, K. *J. Am. Chem. Soc.* **2004**, *126*, 3032–3033.
- (20) Marpu, S.; Hu, Z.; Omary, M. A. *Langmuir* **2010**, *26* (19), 15523–15531.
- (21) Tang, F.; Ma, N.; Tong, L.; He, F.; Li, L. *Langmuir* **2012**, *28*, 883–888.
- (22) Beck, J. B.; Rowan, S. J. *J. Am. Chem. Soc.* **2003**, *125*, 13922–13923.
- (23) Sun, Y.-P.; Zhou, B.; Lin, Y.; Wang, W.; Fernando, K. A. S.; Pathak, P.; Meziani, M. J.; Harruff, B. A.; Wang, X.; Wang, H.; Luo, P. G.; Yang, H.; Kose, M. E.; Chen, B.; Veca, L. M.; Xie, S.-Y. *J. Am. Chem. Soc.* **2006**, *128*, 7756–7757.
- (24) Hu, S.-L.; Niu, K.-Y.; Sun, J.; Yang, J.; Zhao, N.-Q.; Du, X.-W. *J. Mater. Chem.* **2009**, *19* (4), 484–488.
- (25) Mao, Y.; Bao, Y.; Yan, L.; Li, G.; Li, F.; Han, D.; Zhang, X.; Niu, L. *RSC Adv.* **2013**, *3* (16), 5475–5482.
- (26) Zhang, W. F.; Zhu, H.; Yu, S. F.; Yang, H. Y. *Adv. Mater.* **2012**, *24* (17), 2263–2267.
- (27) Bao, L.; Zhang, Z. L.; Tian, Z. Q.; Zhang, L.; Liu, C.; Lin, Y.; Qi, B.; Pang, D. W. *Adv. Mater.* **2011**, *23* (48), 5801–5806.
- (28) Bloksma, M. M.; Bakker, D. J.; Weber, C.; Hoogenboom, R.; Schubert, U. S. *Macromol. Rapid Commun.* **2010**, *31*, 724–728.
- (29) Kunz, W.; Nostro, P. L.; Ninham, B. W. *Curr. Opin. Colloid Interface Sci.* **2004**, *9*, 1–18.
- (30) von Hippel, P. H.; Schleich, T. *Acc. Chem. Res.* **1969**, *2*, 257–265.
- (31) Zhang, Y.; Furyk, S.; Bergbreiter, D. E.; Cremer, P. S. *J. Am. Chem. Soc.* **2005**, *127*, 14505–14510.
- (32) Liu, X.-Y.; Mu, X.-R.; Liu, Y.; Liu, H.-J.; Chen, Y.; Cheng, F.; Jiang, S.-C. *Langmuir* **2012**, *28*, 4867–4876.
- (33) Liu, X.; Cheng, F.; Liu, H.; Chen, Y. *Soft Matter* **2008**, *4*, 1991–1994.
- (34) Suwa, K.; Yamamoto, K.; Akashi, M.; Takano, K.; Tanaka, N.; Kunugi, S. *Colloid Polym. Sci.* **1998**, *276*, 529–533.
- (35) Zhang, J.; Liu, H.-J.; Yuan, Y.; Jiang, S.; Yao, Y.; Chen, Y. *ACS Macro Lett.* **2013**, *2* (1), 67–71.
- (36) Mu, X.-R.; Tong, J.-G.; Liu, Y.; Liu, X.-Y.; Liu, H.-J.; Chen, Y. *Polymer* **2013**, *54* (9), 2341–2346.